

Relativistic mean field theory for deformed nuclei with the pairing correlations

Lisheng Geng^{1,3,*}), Hiroshi Toki^{1,2,**}),
Satoru Sugimoto^{2,***}) , and Jie Meng^{3, †})

¹*Research Center for Nuclear Physics (RCNP), Osaka University,
Ibaraki, Osaka 567-0047, Japan*

²*Institute for Chemical and Physical Research (RIKEN),
Wako, Saitama 351-0198, Japan*

³*School of Physics, Peking University, Beijing 100871, P.R. China*

Abstract

We develop a relativistic mean field (RMF) description of deformed nuclei with the pairing correlations in the BCS approximation. The treatment of the pairing correlations for nuclei with the Fermi surface being close to the threshold of unbound states needs a special attention. To this end, we take the delta function interaction for the pairing interaction with the hope to pick up those states with the wave function being concentrated in the nuclear region and perform the standard BCS approximation for the single particle states generated by the RMF theory with deformation. We apply the RMF + BCS method to the Zr isotopes and obtain a good description of the binding energies and the nuclear radii of nuclei from the proton drip line to the neutron drip line.

*) E-mail address: lsgeng0@rcnp.osaka-u.ac.jp

**) E-mail address: toki@rcnp.osaka-u.ac.jp

***) E-mail address: satoru@riken.go.jp

†) E-mail address: mengj@pku.edu.cn

§1. Introduction

It is our strong desire to treat all the nuclei including the unstable ones from the proton drip line to the neutron drip line. The relativistic mean field (RMF) theory has been used to calculate these nuclei with one parameter set in all the mass regions.^{1),2),3)} We have to include the deformation and the pairing correlations for a suitable description of finite nuclei. There is an extended study of all the even-even mass nuclei in the entire mass region by Hirata et al. including only the deformation.⁴⁾ This calculation provides a good account of all the nuclei and indicate that almost all nuclei except for the ones with most of the magic numbers are deformed. This calculation, however, does not include the pairing correlations, since the conventional BCS treatment with the constant interaction is not able to handle the case, where the Fermi surface is close to the unbound threshold.⁴⁾

The pairing correlations, on the other hand, are treated nicely in the framework of the relativistic Hartree-Bogoliubov (RHB) method by Meng et al.^{5),6)} They can treat nuclei near the unbound threshold in the RHB framework. They solve the RHB equation in the coordinate space with a box boundary condition. This calculation is, however, limited to spherical nuclei. This method has been applied to many proton magic nuclei and able to provide many interesting features as the giant halo where the neutron density distribution extends far away from the nuclear radius. The calculation, however, takes too much time and we are not able to calculate many nuclei in a systematic manner.

Recently, there was an interesting suggestion made by Yadav et al. that the use of the delta function interaction in the BCS formalism with a proper introduction of the box boundary condition can provide a good description of the proton magic nuclei.⁷⁾ The comparison of the calculated results in the RMF+BCS method with those of the RHB framework came out to be very close for these proton magic nuclei with the spherical shape. The justification of this method was provided by Sandulescu et al. by solving the resonance states and taking into account the width effect exactly in the non-relativistic Skyrme Hartree-Fock framework.⁸⁾ It is very interesting, therefore, to use this prescription for deformed nuclei.

The RMF theory was extended to treat deformed nuclei by Gambhir et al.⁹⁾ They expand the nucleon wave functions and the meson mean fields in terms of the harmonic oscillator wave functions. We take this method for the mean field part and replace the BCS part with the constant interaction and the pairing window by the one with the delta function interaction. The fact that we use the nuclear wave functions, in particular, we take the overlap between the occupied and unoccupied states may pick up states in the continuum having wave functions concentrated in the nuclear region. This method, at least, worked for the spherical nuclei and may work also for the deformed case. We mention that

the relativistic Hartree-Bogoliubov theory was worked out using the expansion method for deformed nuclei.¹⁰⁾

In this paper, we formulate the RMF theory with the BCS method for the pairing correlations. In Sec. 2, we provide the RMF formalism with the deformation and the pairing. In Sec. 3, we apply the method to the Zr isotopes from the proton drip line to the neutron drip line. We compare the calculated results with the ones with the spherical shape and without the pairing correlations. In Sect. 4, we provide the summary of the present work.

§2. RMF with deformation and pairing

We write here the formulation of the RMF theory with the deformation and the pairing correlations. We take the model Lagrangian density with nonlinear terms both for σ and ω mesons as described in detail in Ref.,²⁾ which is given by

$$\begin{aligned} \mathcal{L} = & \bar{\psi}(i\gamma^\mu\partial_\mu - M)\psi + \frac{1}{2}\partial_\mu\sigma\partial^\mu\sigma - \frac{1}{2}m_\sigma^2\sigma^2 - \frac{1}{3}g_2\sigma^3 - \frac{1}{4}g_3\sigma^4 - g_\sigma\bar{\psi}\sigma\psi \\ & - \frac{1}{4}\Omega_{\mu\nu}\Omega^{\mu\nu} + \frac{1}{2}m_\omega^2\omega_\mu\omega^\mu + \frac{1}{4}g_4(\omega_\mu\omega^\mu)^2 - g_\omega\bar{\psi}\gamma^\mu\psi\omega_\mu \\ & - \frac{1}{4}R^a{}_{\mu\nu}R^{a\mu\nu} + \frac{1}{2}m_\rho^2\rho_\mu^a\rho^{a\mu} - g_\rho\bar{\psi}\gamma_\mu\tau^a\psi\rho^{\mu a} \\ & - \frac{1}{4}F_{\mu\nu}F^{\mu\nu} - e\bar{\psi}\gamma_\mu\frac{1-\tau_3}{2}A^\mu\psi, \end{aligned} \quad (2.1)$$

where the field tensors of the vector mesons and of the electromagnetic field take the following form:

$$\begin{cases} \Omega_{\mu\nu} = & \partial_\mu\omega_\nu - \partial_\nu\omega_\mu \\ R^a{}_{\mu\nu} = & \partial_\mu\rho_\nu^a - \partial_\nu\rho_\mu^a - 2g_\rho\epsilon^{abc}\rho_\mu^b\rho_\nu^c \\ F_{\mu\nu} = & \partial_\mu A_\nu - \partial_\nu A_\mu \end{cases} \quad (2.2)$$

and other symbols have their usual meaning.

The classical variational principle leads to the Dirac equation:

$$[-i\alpha\nabla + V(\mathbf{r}) + \beta(M + S(\mathbf{r}))] \psi_i = \epsilon_i\psi_i \quad (2.3)$$

for the nucleon spinors and

$$\begin{cases} \{-\Delta + m_\sigma^2\}\sigma(\mathbf{r}) & = -g_\sigma\rho_s(\mathbf{r}) - g_2\sigma^2(\mathbf{r}) - g_3\sigma^3(\mathbf{r}) \\ \{-\Delta + m_\omega^2\}\omega^\mu(\mathbf{r}) & = g_\omega j^\mu(\mathbf{r}) + g_4\omega_\mu^2(\mathbf{r})\omega^\mu(\mathbf{r}) \\ \{-\Delta + m_\rho^2\}\rho^{a\mu}(\mathbf{r}) & = g_\rho j^{a\mu}(\mathbf{r}) \\ -\Delta A^\mu(\mathbf{r}) & = e j_p^\mu(\mathbf{r}) \end{cases} \quad (2.4)$$

for the mesons, where $V(\mathbf{r})$ represents the vector potential:

$$V(\mathbf{r}) = g_\omega\gamma^\mu\omega_\mu(\mathbf{r}) + g_\rho\tau^a\gamma^\mu\rho_\mu^a(\mathbf{r}) + e\frac{1-\tau_3}{2}\gamma^\mu A_\mu(\mathbf{r}) \quad (2.5)$$

and $S(\mathbf{r})$ is the scalar potential

$$S(\mathbf{r}) = g_\sigma \sigma(\mathbf{r}). \quad (2.6)$$

For the mean-field, the nucleon spinors provide the corresponding source terms:

$$\left\{ \begin{array}{l} \rho_s(\mathbf{r}) = \sum_{i=1}^A \bar{\psi}_i \psi_i \\ j^\mu(\mathbf{r}) = \sum_{i=1}^A \bar{\psi}_i \gamma^\mu \psi_i \\ j^{a\mu}(\mathbf{r}) = \sum_{i=1}^A \bar{\psi}_i \gamma^\mu \tau^a \psi_i \\ j_p^\mu(\mathbf{r}) = \sum_{i=1}^A \bar{\psi}_i \gamma^\mu \frac{1 - \tau_3}{2} \psi_i \end{array} \right. \quad (2.7)$$

where the summations are taken over the valence nucleons only. It should be noted that as usual, the present approach neglects the contribution of negative energy states, i.e., no-sea approximation, which means that the vacuum is not polarized. The coupled equations Eqs. (2.3) and (2.4) are non-linear quantum field equations, and their exact solutions are very complicated. So the mean field approximation is generally used: i.e., the meson field operators in Eq. (2.3) are replaced by their expectation values. Then the nucleons move independently in the classical meson fields. The coupled equations are self-consistently solved by iteration.

Symmetries of the system simplify the calculations considerably. In all the applications in this work, we have time reversal symmetry, and there are no currents in the nucleus and therefore the spatial vector components of ω^μ , $\rho^{a\mu}$ and A^μ vanish. One is left with the time-like components ω^0 , ρ^{a0} and A^0 . Charge conservation guarantees that only the 3-component of the isovector ρ^{00} survives.

2.1. Axially symmetric case

The RMF theory was extended to treat deformed nuclei with axially symmetric shapes by Gambhir et al.⁹⁾ To unify the notation, here a brief review of RMF for axially deformed nuclei will be given.

Many deformed nuclei can be described with axially symmetric shapes. In this case, rotational symmetry is broken, and therefore the total angular momentum, j , is no longer a good quantum number. However, the densities are still invariant with respect to a rotation around the symmetry axis, which shall be assumed to be the z -axis in the following. It then turns out to be useful to work with the cylindrical coordinates, $x = r_\perp \cos \varphi$, $y = r_\perp \sin \varphi$ and z . For such nuclei the Dirac equation can be reduced to a coupled set of partial differential equations in the two variables z and r_\perp . In particular, the spinor ψ_i with the index i is now

characterized by the quantum numbers, Ω_i , π_i , and t_i , where $\Omega_i = m_{l_i} + m_{s_i}$ is the eigenvalue of the symmetry operator J_z , π_i is the parity and t_i is the isospin. The spinor can be written in the form

$$\psi_i(\mathbf{r}, t) = \begin{pmatrix} f_i(\mathbf{r}) \\ ig_i(\mathbf{r}) \end{pmatrix} = \frac{1}{\sqrt{2\pi}} \begin{pmatrix} f_i^+(z, r_\perp) e^{i(\Omega_i-1/2)\varphi} \\ f_i^-(z, r_\perp) e^{i(\Omega_i+1/2)\varphi} \\ ig_i^+(z, r_\perp) e^{i(\Omega_i-1/2)\varphi} \\ ig_i^-(z, r_\perp) e^{i(\Omega_i+1/2)\varphi} \end{pmatrix} \chi_{t_i}(t). \quad (2.8)$$

The four components $f_i^\pm(r_\perp, z)$ and $g_i^\pm(r_\perp, z)$ obey the coupled Dirac equations. For each solution with positive Ω_i , ψ_i , we have the time-reversed solution with the same energy, $\psi_{\bar{i}} = T\psi_i$, with the time reversal operator, $T = -i\sigma_y K$ (K being the complex conjugation). For nuclei with time reversal symmetry, the contributions to the densities of the two time reversed states i and \bar{i} are identical. Therefore, we find the densities

$$\rho_{s,v} = 2 \sum_{i>0} ((|f_i^+|^2 + |f_i^-|^2) \mp (|g_i^+|^2 + |g_i^-|^2)) \quad (2.9)$$

and, in a similar way, ρ_3 and ρ_c . The sum $i > 0$ runs only over the states with positive Ω_i -values. These densities serve as sources for the fields $\phi = \sigma, \omega^0, \rho^{00}$, and A^0 , which are determined by the Klein-Gordon equation in cylindrical coordinates.

For the solution of the RMF equations the basis expansion method is used. We follow closely the details, presentation and the notations of ref.¹¹⁾ For the axially symmetric case the spinors, f_i^\pm and g_i^\pm , in Eq. (2.8) are expanded in terms of the eigenfunctions of a deformed axially symmetric oscillator potential.

$$V_{osc}(z, r_\perp) = \frac{1}{2} M \omega_z^2 z^2 + \frac{1}{2} M \omega_{r_\perp}^2 r_\perp^2 \quad (2.10)$$

Imposing volume conservation, the two oscillator frequencies ω_\perp and ω_z can be expressed in terms of a deformation parameter, β_0 : $\omega_z = \omega_0 \exp\left(-\sqrt{\frac{5}{4\pi}}\beta_0\right)$, and $\omega_\perp = \omega_0 \exp\left(+\frac{1}{2}\sqrt{\frac{5}{4\pi}}\beta_0\right)$.

The basis is now determined by the two constants ω_0 and β_0 . The eigenfunctions of the deformed harmonic oscillator potential are characterized by the quantum numbers, $|\alpha\rangle = |n_z, n_r, m_l, m_s\rangle$, where m_l and m_s are the components of the orbital angular momentum and of the spin along the symmetry axis. The eigenvalue of J_z , which is a conserved quantity in these calculations, is $\Omega = m_l + m_s$. The parity is given by $\pi = (-)^{n_z+m_l}$.

The eigenfunctions of the deformed harmonic oscillator can be written explicitly as

$$\Phi_\alpha(z, r_\perp, \varphi, s, t) = \phi_{n_z}(z) \phi_{n_r}^{m_l}(r_\perp) \frac{1}{\sqrt{2\pi}} e^{im_l\varphi} \chi_{m_s}(s) \chi_{t_\alpha}(t) \quad (2.11)$$

with

$$\begin{aligned}\phi_{n_z}(z) &= \frac{N_{n_z}}{\sqrt{b_z}} H_{n_z}(\zeta) e^{-\zeta^2/2} \\ \phi_{n_r}^{m_l}(r_\perp) &= \sqrt{2} \frac{N_{n_r}^{m_l}}{b_\perp} \eta^{m_l/2} L_{n_r}^{m_l}(\eta) e^{-\eta/2},\end{aligned}\tag{2.12}$$

where $\zeta = z/b_z$ and $\eta = r_\perp^2/b_\perp^2$. The polynomials $H_n(\zeta)$ and $L_n^m(\eta)$ are Hermite polynomials and associated Laguerre polynomials as defined in Ref.¹²⁾ N 's are the normalization constants.

The spinors f_i^\pm and g_i^\pm in Eq. (2.8) are explicitly given by the following relations

$$\begin{cases} f_i^+(z, r_\perp) &= \sum_{\alpha}^{\alpha_{max}} f_{\alpha}^{(i)} \phi_{n_z}(z) \phi_{n_r}^{(\Omega-1/2)}(r_\perp) \\ f_i^-(z, r_\perp) &= \sum_{\alpha}^{\alpha_{max}} f_{\alpha}^{(i)} \phi_{n_z}(z) \phi_{n_r}^{(\Omega+1/2)}(r_\perp) \\ g_i^+(z, r_\perp) &= \sum_{\beta}^{\beta_{max}} g_{\beta}^{(i)} \phi_{n_z}(z) \phi_{n_r}^{(\Omega-1/2)}(r_\perp) \\ g_i^-(z, r_\perp) &= \sum_{\beta}^{\beta_{max}} g_{\beta}^{(i)} \phi_{n_z}(z) \phi_{n_r}^{(\Omega+1/2)}(r_\perp) \end{cases}\tag{2.13}$$

The quantum numbers α_{max} and β_{max} are chosen in such a way that the corresponding major quantum numbers $N = n_z + 2n_\rho + m_l$ are not larger than $N_F + 1$ for the expansion of the small components, and not larger than N_F for the expansion of the large components.

2.2. Pairing with delta function interaction

Based on the single-particle spectrum calculated by the RMF method described above, we perform a state-dependent BCS calculations.^{13), 14)} The gap equation has a standard form for all the single particle states. i.e.

$$\Delta_k = \frac{1}{2} \sum_{k' > 0} \frac{\bar{V}_{kk'} |\Delta_{k'}|}{\sqrt{(\varepsilon_{k'} - \lambda)^2 + \Delta_{k'}^2}},\tag{2.14}$$

where $\varepsilon_{k'}$ is the single particle energy and λ is the Fermi energy, whereas the particle number condition is given by $2 \sum_{k > 0} v_k^2 = N$. In the present work we use for the pairing interaction a delta force, i.e.,

$$V = -V_0 \delta(\mathbf{r}_1 - \mathbf{r}_2)\tag{2.15}$$

with the same strength V_0 for both protons and neutrons. Apart from its simplicity, the applicability and justification of using such a δ -function has been recently discussed in¹⁵⁾ and references therein, whereby it has been shown in the context of HFB calculations that the use of a delta force in finite space simulates the effect of finite range interaction in a phenomenological manner. The pairing matrix element for the δ -function force is given by

$$\bar{V}_{ij} = \langle i\bar{i} | V | j\bar{j} \rangle - \langle i\bar{i} | V | \bar{j}j \rangle = -V_0 \int d^3r \left[\psi_i^\dagger \psi_i^\dagger \psi_j \psi_{\bar{j}} - \psi_i^\dagger \psi_i^\dagger \psi_{\bar{j}} \psi_j \right]\tag{2.16}$$

with the pairing energy defined by $E_{pair} = -\sum_{k>0} \Delta_k u_k v_k$. Eq. (2.3), Eq. (2.4), the gap equations (2.14) and the total particle number N for a given nucleus are self-consistently solved by iteration.

§3. Numerical calculation for Zr isotopes

We apply the formalism to the Zr isotopes from the proton drip line to the neutron drip line. For the RMF Lagrangian, we take the A-dependent parameter set TMA.^{2),17),16)} The parameter values are given below. The mass of nucleon, and that of σ , ω and ρ mesons are, respectively, $M = 938.900$ MeV, $m_\sigma = 519.151$ MeV, $m_\omega = 781.950$ MeV, $m_\rho = 768.100$ MeV. The effective strengths of the coupling between various mesons and nucleons have the values $g_\sigma = 10.055 + 3.050/A^{0.4}$, $g_\omega = 12.842 + 3.191/A^{0.4}$ and $g_\rho = 3.800 + 4.644/A^{0.4}$. The nonlinear coupling strength of the σ meson are given by $g_2 = -0.328 - 27.879/A^{0.4}$ (fm⁻¹), and $g_3 = 38.862 - 184.191/A^{0.4}$, whereas the self coupling of the ω field has the strength $g_4 = 151.590 - 378.004/A^{0.4}$. As for the pairing interaction, we take the strength of the delta function interaction as $V_0 = -343.7$ MeV fm⁻³, which is fixed by requiring that the experimental value of the proton pairing gap in ⁹⁰Zr (1.714 MeV) is reproduced within a given energy cut-off ($E_{max} - \lambda \leq 8.0$ MeV).

Since in many nuclei we have several solutions at different equilibrium deformations with similar energies, it is difficult to select the ground-state configuration uniquely. What we decide to do here is as follows. First we take the results of the constrained calculations¹⁸⁾ on the quadrupole moment, Q_{20} , to obtain all possible ground state configuration in the framework of RMF.⁴⁾ We will see later that the deformation parameters from RMF calculations are indeed good guesses even after the pairing interaction is included. Second we perform non-constrained calculations in the RMF+BCS framework starting from the deformation parameter of the deepest minimum of the energy curve of each nucleus as an initial guess and obtain the deformation and other observables as final values.

In the calculation of the Zr isotopes, the number of shells taken into account is 14 for both fermions and bosons. Following Ref.,⁹⁾ we fix $\hbar\omega_0 = 41A^{-1/3}$ for fermions. In what follows we discuss the details of our calculations and the numerical results for the Zr isotopes.

3.1. Binding energy per nucleon and two neutron separation energy

The two neutron separation energy, S_{2n} , defined as,

$$S_{2n}(Z, N) = B(Z, N) - B(Z, N - 2), \quad (3.1)$$

is quite a sensitive quantity to test a microscopic theory, where $B(Z, N)$ are the binding energies of nuclei with the proton number, Z , and the neutron number, N . The two neutron

Table I. The ground state properties of even Zr isotopes calculated with the parameter set TMA.

Listed are B_{tot} total binding energy, B_{per} binding energy per nucleon, charge(R_c), neutron(R_n), proton(R_p), and matter(R_m) root mean square radii as well as quadrupole deformation parameter for neutron(β_{2n}), proton(β_{2p}) and matter(β_{2m}) distribution with A as mass number and N as neutron number

A	N	B_{tot}	B_{per}	R_c	R_n	R_p	R_m	β_{2n}	β_{2p}	β_{2m}
78	38	639.089	8.193	4.3331	4.1496	4.2586	4.2058	0.480	0.507	0.494
80	40	667.668	8.346	4.3431	4.2048	4.2688	4.2369	0.489	0.506	0.498
82	42	692.014	8.439	4.4085	4.3134	4.3353	4.3241	0.589	0.579	0.584
84	44	716.742	8.533	4.2734	4.2081	4.1979	4.2033	-0.205	-0.210	-0.207
86	46	739.502	8.599	4.2694	4.2381	4.1938	4.2175	-0.148	-0.166	-0.156
88	48	762.784	8.668	4.2628	4.2618	4.1871	4.2280	0.002	0.003	0.002
90	50	784.859	8.721	4.2697	4.2969	4.1941	4.2515	0.000	0.000	0.000
92	52	797.819	8.672	4.3056	4.3678	4.2307	4.3087	-0.121	-0.137	-0.128
94	54	811.838	8.637	4.3504	4.4372	4.2762	4.3695	0.216	0.226	0.220
96	56	825.419	8.598	4.3832	4.5023	4.3095	4.4230	0.267	0.269	0.268
98	58	837.427	8.545	4.5171	4.6629	4.4456	4.5755	0.525	0.517	0.522
100	60	849.997	8.500	4.4694	4.6457	4.3972	4.5480	0.412	0.393	0.405
102	62	860.800	8.439	4.4896	4.6945	4.4177	4.5880	0.407	0.391	0.401
104	64	870.744	8.373	4.5117	4.7424	4.4402	4.6285	0.406	0.395	0.402
106	66	879.994	8.302	4.5357	4.7903	4.4646	4.6701	0.409	0.403	0.407
108	68	888.649	8.228	4.5579	4.8366	4.4872	4.7102	0.408	0.407	0.408
110	70	895.861	8.144	4.5930	4.8991	4.5228	4.7657	0.442	0.435	0.440
112	72	902.253	8.056	4.6302	4.9699	4.5606	4.8277	0.501	0.466	0.488
114	74	910.199	7.984	4.5182	4.9054	4.4468	4.7496	-0.169	-0.173	-0.170
116	76	916.310	7.899	4.5284	4.9396	4.4571	4.7788	-0.142	-0.156	-0.147
118	78	922.451	7.817	4.5189	4.9614	4.4475	4.7934	0.001	0.000	0.000
120	80	928.345	7.736	4.5364	4.9908	4.4653	4.8220	-0.001	-0.001	-0.001
122	82	933.816	7.654	4.5542	5.0184	4.4834	4.8495	0.000	0.000	0.000
124	84	933.842	7.531	4.5653	5.0909	4.4947	4.9065	-0.014	-0.009	-0.013
126	86	934.295	7.415	4.5980	5.1619	4.5279	4.9694	0.162	0.115	0.147
128	88	935.359	7.307	4.6488	5.2217	4.5794	5.0298	0.237	0.204	0.227
130	90	936.150	7.201	4.6746	5.2808	4.6057	5.0826	0.261	0.228	0.251
132	92	937.086	7.099	4.6606	5.3443	4.5914	5.1278	-0.232	-0.184	-0.218
134	94	937.686	6.998	4.6787	5.3932	4.6098	5.1718	-0.239	-0.188	-0.224
136	96	937.995	6.897	4.6960	5.4382	4.6274	5.2128	-0.241	-0.190	-0.226
138	98	938.148	6.798	4.7133	5.4808	4.6449	5.2522	-0.243	-0.190	-0.227
140	100	937.988	6.700	4.7314	5.5211	4.6632	5.2902	-0.244	-0.192	-0.229

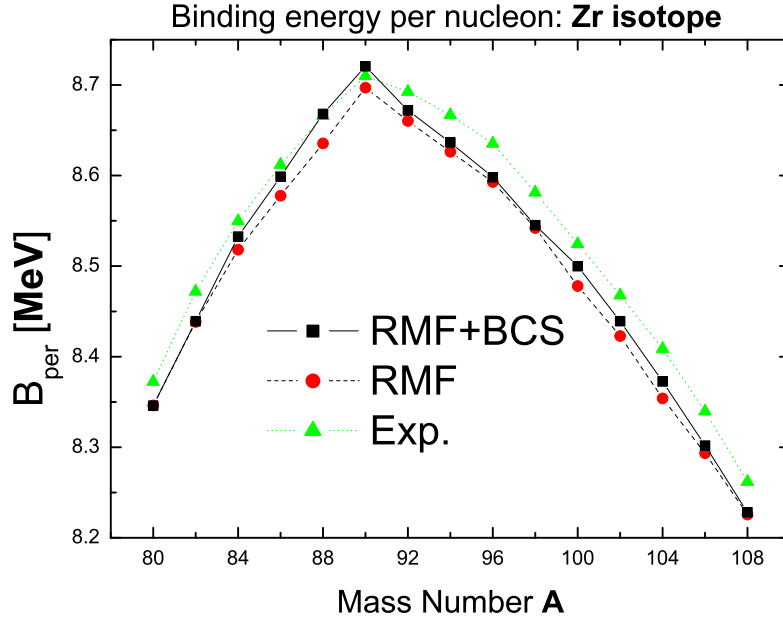


Fig. 1. Binding energy per nucleon B_{per} of even Zr isotopes are plotted as a function of mass number A , for the deformed RMF+BCS calculations (square), the deformed RMF calculations (circle) and the experimental data¹⁹⁾ (triangle).

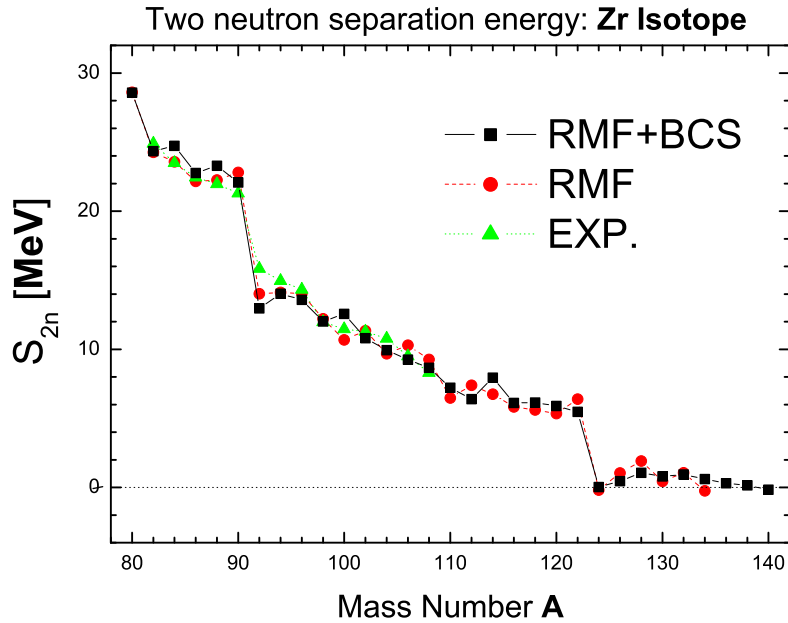


Fig. 2. Two neutron separation energies, S_{2n} , of even Zr isotopes are plotted as a function of mass number A , for the deformed RMF+BCS calculations (square), the deformed RMF calculations (circle) and the experimental data¹⁹⁾ (triangle).

separation energy becomes negative when the nucleus becomes unstable against the two neutron emission. Hence, the drip line nucleus for a corresponding isotope chain is the one before the nucleus with the negative S_{2n} .

In Fig. 1 and Fig. 2, we plot the results of binding energy per nucleon $^{80-100}\text{Zr}$ and the results of two-neutron separation energies for the entire chain of Zr isotopes covering the proton and neutron drip-lines. The figure also shows the results of RMF calculations and the available experimental data.¹⁹⁾ First, from Fig. 1, we can see RMF+BCS give a better description of binding energy per nucleon than RMF calculations. The largest difference between RMF+BCS and the experimental value is less than 0.04 MeV. If we notice here most of nuclei are deformed and we do not readjust any parameter for our calculations, the agreement is really remarkable. Second, from Fig. 2, we see basically a good agreement between experiment and the present calculation. The so-called giant-halos²⁰⁾ ($^{124}\text{Zr} \sim ^{138}\text{Zr}$) are well reproduced. The strong variation in the experimental separation energy at the neutron magic number $N = 50$ is well accounted for by the present calculation. There is a sudden increase for ^{114}Zr which can be explained by the deformation effect. As we can see from Table. I and Fig. 6, for ^{112}Zr , $\beta_{2m} \approx 0.5$, while for ^{124}Zr , $\beta_{2m} \approx -0.2$. With the assumption of spherical shapes, Ref.²⁰⁾ predicted that the drip-line nuclei for Zr isotopes is ^{140}Zr . We obtain also the drip-line nuclei being predicted to be ^{140}Zr .

3.2. Root mean square neutron radii

The root mean square neutron radii are other important basic physical quantities to describe the neutron-rich nuclei as well as the two neutron separation energies. In the mean field theory, the root mean square (rms) neutron radii can be directly deduced from the neutron density distributions, ρ_n :

$$R_n = \langle r_n^2 \rangle^{1/2} = \left\{ \frac{\int \rho_n r^2 d\mathbf{r}}{\int \rho_n d\mathbf{r}} \right\}^{1/2} \quad (3.2)$$

In Fig. 3, the root mean square neutron radii of Zr nuclei are presented. Although calculation is done with the assumption of spherical shapes, the results of RCHB²⁰⁾ are also shown as comparison. Two interesting features are clearly seen. First, the so-called giant-halos²⁰⁾ are obtained ($^{124}\text{Zr} \sim ^{138}\text{Zr}$). Second, nuclei with large absolute β_{2m} values (see Table. I and Fig. 6) tend to have larger rms neutron radii, $^{78}\text{Zr} \sim ^{82}\text{Zr}$ and $^{94}\text{Zr} \sim ^{112}\text{Zr}$. This can also be seen from the fact that some RMF results (^{100}Zr and ^{126}Zr) are larger than RMF+BCS results.

Another thing we note here is, despite of the second effect mentioned above, for the so-called giant-halos, the present work gives relatively small values for the root mean square neutron radii. This should be due to the harmonic oscillator basis we take for the calculations

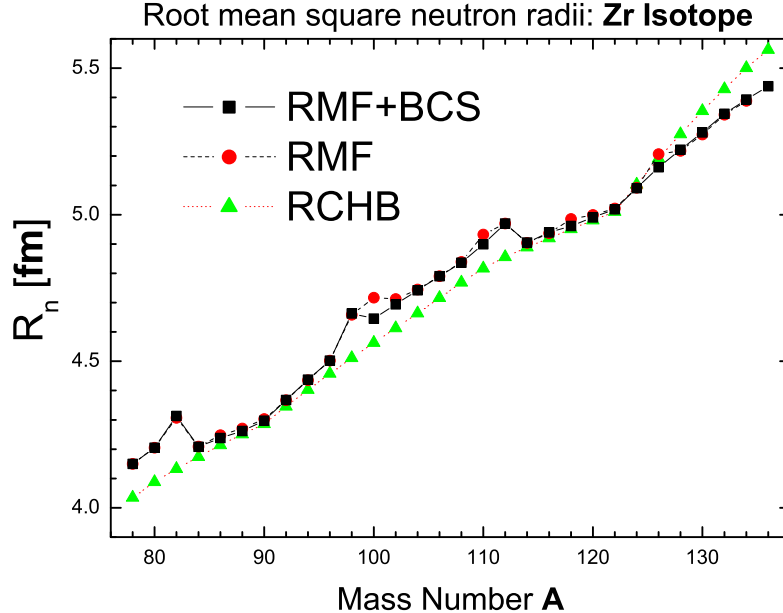


Fig. 3. The root mean square neutron radii in even Zr isotopes are plotted as a function of mass number, A , for the deformed RMF+BCS calculation (square), the deformed RMF calculation (circle), and the spherical RCHB calculation²⁰⁾ (triangle).

of the deformed nuclei. This deficiency will be worked out in the near future, although a lot of effort is necessary to change the numerical method. Nevertheless, despite of the small discrepancies for giant-halos, the present work provides a good agreement with the RCHB²⁰⁾ results and can give a reliable prediction of rms neutron radii to all the nuclei from the proton drip-line to the neutron drip-line.

3.3. Single particle states and their occupation probabilities

One interesting feature of exotic nuclei is the contribution from the continuum due to the pairing correlations. In this context, it is definitely very interesting to see how different are the contributions from the continuum between the calculations with constant pairing interactions and the calculations with delta function interaction. We present the occupation probabilities of neutron single particle states for two cases; the delta function interaction and the constant pairing interaction usually used in the BCS framework. In the constant pairing calculation, we take $G_n = 12.0/A$ and $G_p = 30.0/A$, where A is the mass number of ^{124}Zr , and the pairing window as $\varepsilon_i - \lambda \leq 2(41A^{-1/3})$.⁹⁾ Here, we take different pairing strengths, G , for protons and neutrons in order to get similar gap energies, Δ , with the ones of the delta function interaction. In Fig. 4, we show the occupation probabilities of ^{124}Zr for the neutron levels near the Fermi surface, i.e., in the interval $-10 \leq E_{s,p} \leq 8$ MeV. The results

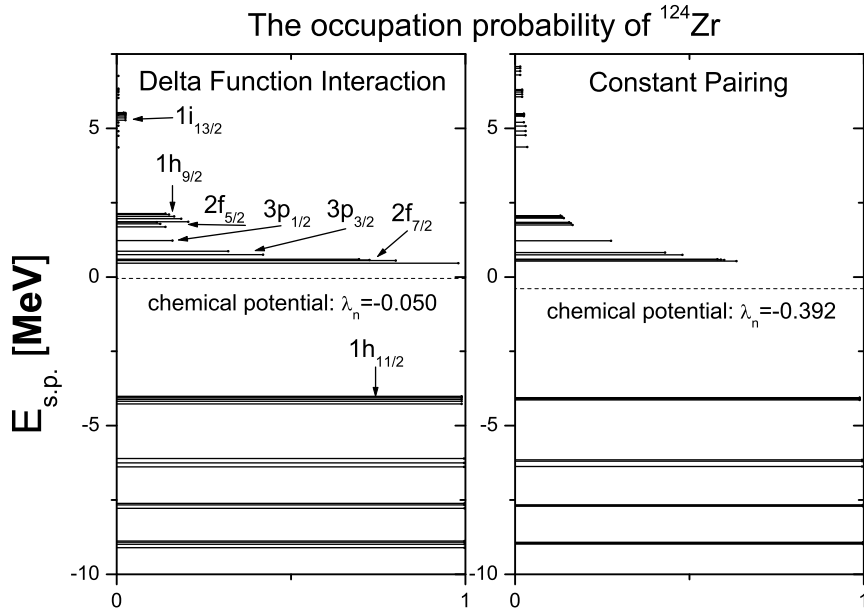


Fig. 4. The occupation probability is shown by solid horizontal bar for each neutron single particle state in ^{124}Zr . The left panel is the result of the BCS calculation with the delta function interaction, while the right panel is the result of constant pairing calculation. The dotted horizontal line represents the Fermi energy. In both panels, the occupation probabilities of the continuum states are multiplied by a factor of 5 for guiding eyes.

of delta function interaction and constant pairing calculations are plotted respectively on the left and right panels. Since in our calculation, ^{124}Zr is almost spherical, we denote the corresponding spherical quantum number on the left panel. We see all the spherical shell model states with small spin-orbit splitting in the positive energy region. They are all resonance states supported by the centrifugal potential. A recent resonant RMF+BCS calculation²¹⁾ shows a quite similar spectra for ^{124}Zr . It is seen that the contributions from the continuum states are very important. We see clearly that the BCS calculation with the delta function interaction can pick up more the continuum states which has larger localization within the nuclear region, which correspond to resonance states. While in the constant pairing case, the occupation probabilities decrease monotonously with increasing single particle energy. To see this point more clearly, we plot the corresponding resonant wave function f in Fig. 5. It is easily seen that these states do have similar behaviors as bound states.

We point out an interesting feature of the vacancy between $E \approx 2\text{MeV}$ and $E \approx 5\text{MeV}$ in the single particle spectra in the continuum seen in both calculations. If we perform calculations of the single particle states in the coordinate space using the box boundary

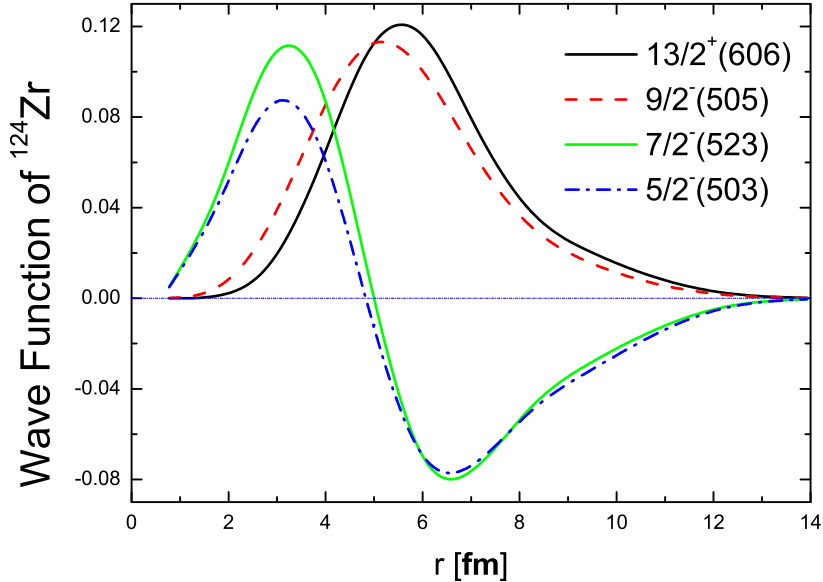


Fig. 5. The wavefunction $f(z, r_{\perp})$ of four typical resonant states in ^{124}Zr are plotted as a function of r_{\perp} at $z = 0.422$. The corresponding energy (in MeV) and occupation probabilities are respectively $13/2^+(606) : E = 5.276, v^2 = 0.005$; $9/2^-(505) : E = 1.857, v^2 = 0.041$; $7/2^-(523) : E = 0.464, v^2 = 0.196$ and $5/2^-(503) : E = 1.683, v^2 = 0.028$.

condition instead of the harmonic oscillator expansion method, we would get many states in the continuum. They are so called scattering states, which have small probabilities in the nuclear region. We do not get these scattering states at least in the region of several MeV excitation energy in the continuum. Hence, those single particle states near the continuum threshold do have large probabilities in the nuclear region and contribute to the pairing correlations in the nuclei close to the neutron drip line.

This unique feature of the delta function interaction in the BCS method is essential for the study of the drip-line nuclei, where the Fermi energy is close to the threshold to the continuum. In this case, we have to estimate correctly the coupling between the bound states and the continuum states in order to pick up the resonance states, which have large amplitudes in the nuclear region. This would justify us to use such a simple RMF+BCS model to study all the nuclei including the unstable ones from the proton drip-line to the neutron drip-line as already demonstrated for the spherical case by Yadav et al.⁷⁾

3.4. Effect of pairing on the deformation

The quadrupole moments of proton, neutron and nucleon distributions are calculated by

$$\begin{aligned} Q_i &= \sqrt{\frac{16\pi}{5}} \langle r^2 Y_{20}(\theta) \rangle_i \\ &= \langle 2z^2 - x^2 - y^2 \rangle_i, \end{aligned} \quad (3.3)$$

where Y_{lm} is the spherical harmonics with l being multi-polarity. The index $i = p, n, m$ denotes the expectation values with respect to the proton, neutron and nucleon distributions, respectively.

The deformation parameters are defined in terms of the liquid drop model with uniform density. We expand the sharp surface of the liquid drop as

$$R_i(\theta) = R_0 [1 + \beta_{2i} Y_{20}(\theta) + \beta_{4i} Y_{40}(\theta)], \quad (3.4)$$

where $R_0 = 1.2A^{1/3}$ fm, in terms of the spherical harmonics under the axial symmetry. The quadrupole moment of nucleon distribution in the liquid model is calculated as

$$Q_m^{liq} = \sqrt{\frac{16\pi}{5}} \frac{3A}{4\pi} R_0^2 \beta_{2m} \quad (3.5)$$

dropping the higher order terms of $\beta_{\lambda m}$. The deformation parameter, β_{2m} , is determined such that Q_m^{liq} reproduces Q_m in the RMF calculation and is given by

$$\begin{aligned} \beta_{2m} &= \frac{\sqrt{5\pi}}{3} \frac{1}{AR_0^2} Q_m \\ &= \frac{\sqrt{5\pi}}{3} \frac{1}{AR_0^2} \langle 2z^2 - x^2 - y^2 \rangle_m \end{aligned} \quad (3.6)$$

The deformation parameters, β_{2p} and β_{2n} , are similarly given by

$$\beta_{2p} = \frac{\sqrt{5\pi}}{3} \frac{1}{ZR_0^2} Q_p \quad (3.7)$$

$$\beta_{2n} = \frac{\sqrt{5\pi}}{3} \frac{1}{NR_0^2} Q_n \quad (3.8)$$

In the above procedure to extract $\beta_{\lambda i}$, we keep the linear relations between the moments and the deformation parameters so that one can easily reproduce the moments from the deformation parameters in the tabulation. As for the determination of the deformation parameters keeping higher order of terms of $\beta_{\lambda i}$, we refer the description in Ref.²²⁾

We show in Fig.6, the quadrupole deformation, β_{2m} , for both the deformed RMF calculation and the deformed RMF+BCS calculation. It is easily seen that the pairing effect

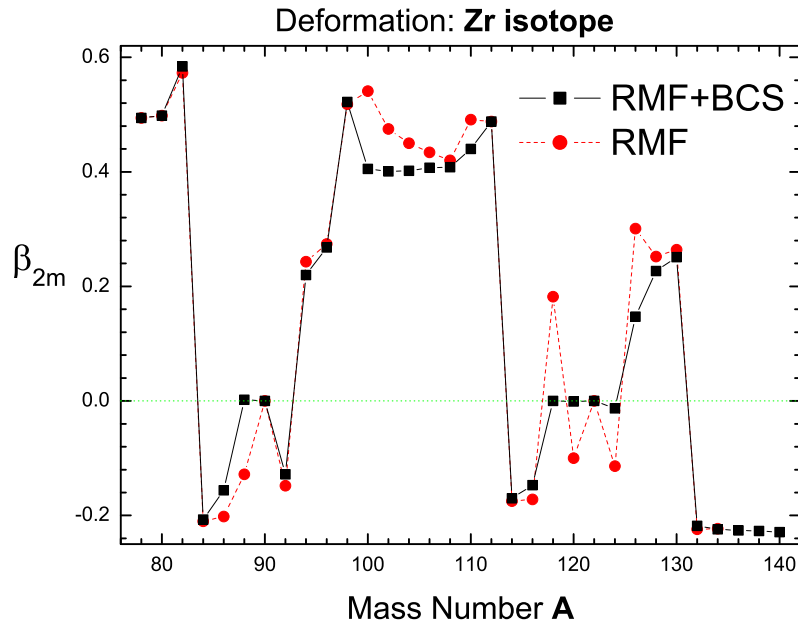


Fig. 6. The quadrupole deformation β_{2m} for the Zr isotopes obtained from the deformed RMF+BCS (square) and the deformed RMF (circle) calculations.

can reduce the deformation of nuclei. More specifically, for some nuclei whose $|\beta_{2m}| < 0.2$ in the RMF calculation, i.e., ^{88}Zr and $^{118}\text{Zr} \sim ^{124}\text{Zr}$, the deformations are removed almost completely. While for other largely deformed nuclei ($\beta_{2m} > 0.3$), β_{2m} are reduced somewhat, although not so much as their weakly deformed counterparts.

§4. Conclusion

We have formulated the RMF theory with deformation and pairing. Deformed nuclei are calculated usually using the expansion method in terms of the harmonic oscillator wave functions with the pairing correlations being treated using the constant pairing with pairing window. This method is, however, not applicable for the case of nuclei close to the neutron and proton drip lines due to the increasing importance of the resonance states in the continuum. We have introduced therefore the delta function interaction for the pairing interaction with the hope to introduce the state dependence to the pairing matrix elements, since the delta function description was demonstrated to work for the spherical nuclei.

In this paper, to demonstrate the method is applicable, we have applied the RMF method with the delta function interaction to the Zr isotopes from the proton drip line to the neutron drip line with the deformation. We have calculated the binding energies, the neutron radii, the deformations and the gap energies of these nuclei. We have shown the two neutron

separation energies as a function of the mass number. The comparison of the present results with experimental separation energies is good for the two neutron separation energies. The effect of deformation is visible in this quantity due to the large variation of the deformation as a function of the mass number. The neutron radii increase monotonically with the neutron number with some anomalies when the deformation changes suddenly. The so-called giant halo effect is preserved for the nuclei close to the neutron drip line.

The occupation probabilities in the continuum are important quantities to show the present pairing treatment effective for the treatment of the pairing in the continuum. While the occupation probabilities drop monotonically as the states deviate from the Fermi energy for the case of the constant pairing interaction, they show the characteristic behavior for the case of the delta function interaction. The occupation probabilities are large for those states, whose wave functions have large overlap with the wave functions below the Fermi surface. It would be interesting to compare with the results of the Hartree-Bogoliubov calculations for these nuclei.

The deformation varies largely for the Zr isotopes. The pairing correlations have an effect to reduce the deformation, which is clearly seen in our calculations. For those nuclei having small deformations when calculated without pairing, the pairing correlations make the nuclei spherical.

We have calculated the Zr isotopes to demonstrate the present RMF method with the deformation and the pairing correlations even for nuclei close to the drip lines. It is very interesting to calculate many nuclei in the whole mass regions with the present method.

§5. Acknowledgments

We acknowledge fruitful discussions and collaborations with Prof. N. Sandulescu on the treatment of pairing in the continuum.

References

- 1) D. Hirata, H. Toki, T. Watabe, I. Tanihata, B.V. Carlson, Phys. Rev. C44 (1991), 1467.
- 2) Y. Sugahara and H. Toki, Nucl. Phys. **A579** (1994), 557.
- 3) P. Ring, Prog. Part. Nucl. Phys. **37** (1996), 193.
- 4) D. Hirata, K. Sumiyoshi, I. Tanihata, Y. Sugahara, T. Tachibana and H. Toki, Nucl. Phys. **A616** (1997), 438c, and D. Hirata, K. Sumiyoshi, I. Tanihata, Y. Sugahara, and H. Toki, *RIKEN-AF-NP-268* (1997).
- 5) J. Meng, and P. Ring, Phys. Rev. Lett. **77** (1996), 3963.

- 6) J. Meng, Nucl. Phys. **A635** (1998), 3.
- 7) H. L. Yadav, S. Sugimoto and H. Toki, Mod. Phys. Lett **A17** (2002), 2523.
- 8) N. Sandulescu, Nguyen Van Giai, and R. J. Liotta, Phys. Rev. **C61** (2000), 061301(R)
- 9) Y.K. Gambhir, P. Ring and A. Thimet, Ann. Phys. (N.Y.) **194** (1990), 132.
- 10) G.A. Lalazissis, D. Vretenar, and P. Ring, Nucl. Phys. **A650** (1999), 133.
- 11) P. Ring, Y.K. Gambhir and G.A. Lalazissis, Comput. Phys. Commun, 105 (1997), 77.
- 12) M. Abramowitz and I. A. Stegun, *Handbook of Mathematical Functions*, Dover, New York, 1970.
- 13) A. M. Lane, *Nuclear Theory* (Benjamin, 1964).
- 14) P. Ring and P. Schuck, *The Nuclear Many-Body Problem* (Springer, 1980).
- 15) J. Dobaczewski, W. Nazarewicz, T. R. Werner, J. F. Berger, C. R. Chinn, and J. Dechargé, Phys. Rev. **C53** (1996), 2809.
- 16) Y. Sugahara, Doctor thesis in Tokyo Metropolitan University (1995).
- 17) H. Toki, D. Hirata, Y. Sugahara, K. Sumiyoshi and I. Tanihata, Nucl. Phys. **A588** (1995), 357c.
- 18) F. Floard et al., Nucl. Phys. **A203** (1973), 433.
- 19) G. Audi and A. H. Wapstra, Nucl. Phys. **A595** (1995), 409.
- 20) J. Meng and P. Ring, Phys. Rev. Lett. **80** (1998), 460.
- 21) N. Sandulescu, L.S. Geng, H. Toki, and G. Hillhouse, *arXiv:nucl-th/0306035*
- 22) N. Tajima, S. Takahara and N. Onishi, Nucl. Phys. **A603** (1996), 23